



# Data-based estimates of ocean carbon uptake biased high from neglect of submonthly atmospheric pressure variability

Jeanne Dombret<sup>1</sup>, Hugo Bellenger<sup>1</sup>, Xavier Perrot<sup>1</sup>, Laëticia Parc<sup>1</sup>, Lester Kwiatkowski<sup>2</sup>, Frédéric Chevallier<sup>3</sup>, Laurent Bopp<sup>1</sup>, Marion Gehlen<sup>3</sup>, Roland Séférian<sup>4</sup>, Sarah Berthet<sup>4</sup>, and James C. Orr<sup>3</sup>

<sup>1</sup>Laboratoire de Météorologie Dynamique, LMD-IPSL, École Normale Supérieure, Université PSL, École polytechnique, Institut Polytechnique de Paris, Sorbonne Université, CNRS, Paris France

<sup>2</sup>Laboratoire d'Océanographie et du Climat: Expérimentations et Approches Numériques, LOCEAN-IPSL, Sorbonne Université-CNRS-IRD-MNH, Paris, France

<sup>3</sup>Laboratoire des Sciences du Climat et de l'Environnement, LSCE-IPSL, CEA-CNRS-UVSQ, Université Paris Saclay, Gif-sur-Yvette, France

<sup>4</sup>Centre National de Recherches Météorologiques (CNRM), Université de Toulouse, Météo-France, CNRS, Toulouse, France

**Correspondence:** Hugo Bellenger (hugo.bellenger@lmd.ipsl.fr)

Received: 20 October 2025 – Discussion started: 17 December 2025

Revised: 16 April 2026 – Accepted: 12 May 2026 – Published: 23 June 2026

**Abstract.** Current estimates of the global ocean carbon sink based on measurements of CO<sub>2</sub> fugacity are inconsistent with those obtained from global ocean biogeochemistry models. Here we investigate how this gap might change by more fully accounting for submonthly variability in observation-based estimates, a step closer to the roughly hourly frequencies used in models. While these data-based estimates use hourly to 6-hourly wind speeds to compute the air-sea CO<sub>2</sub> flux, other input variables are available only at monthly resolution. Thus, they neglect high-frequency variability in key variables such as atmospheric pressure associated with synoptic events such as storms. To evaluate this error, we compare flux estimates from observational data sets with different temporal resolutions. Accounting for hourly variations in atmospheric pressure and daily variations in sea surface temperature, a data-based approach reduces the estimated global carbon uptake by 0.12 Pg C yr<sup>-1</sup>, closing 25 % of the average gap between observation-based and model estimates. This reduction results from proper accounting of the covariance between wind speed and atmospheric pressure, particularly in the southern extratropics.

*Key points.*

- Neglect of submonthly variability of atmospheric pressure in data-based ocean carbon sink estimates causes a positive bias of 0.12 Pg C yr<sup>-1</sup>
- This bias represents on average 25 % of the gap between model and data-based estimates of the sink between 2008 and 2019
- This bias is driven by the covariance between wind speed and atmospheric pressure, 85 % of which stems from the southern midlatitudes

## 1 Introduction

The ocean absorbs one-fourth of anthropogenic CO<sub>2</sub> emissions, playing a major role in the global carbon cycle. It is estimated to have absorbed 2.9 Pg C yr<sup>-1</sup> of anthropogenic carbon during 2014–2023 based on the Global Carbon Budget (GCB, Friedlingstein et al., 2025). But this average value comes with a spread of more than 1 Pg C yr<sup>-1</sup> between the lowest and highest estimates. The GCB is updated annually to reflect the evolution in the data and methods used to obtain the latest estimates of global carbon emissions and carbon storage in different reservoirs (sinks). Its ocean estimate relies on two different approaches.

The first approach uses global ocean biogeochemistry models (GOBMs), each of which couples a global-scale, general ocean circulation model to an ocean carbon cycle com-

ponent. GOBMs simulate ocean transport of dissolved inorganic carbon (DIC) and total alkalinity (Alk), from which is calculated surface ocean CO<sub>2</sub> fugacity ( $f\text{CO}_{2\text{sea}}$ ), a variable nearly identical to the ocean partial pressure of CO<sub>2</sub> ( $p\text{CO}_{2\text{sea}}$ ). From that, the models compute the difference relative to the atmospheric CO<sub>2</sub> fugacity ( $f\text{CO}_{2\text{atm}}$ ), multiplying that difference by a gas transfer velocity times the solubility to compute the air-sea CO<sub>2</sub> flux. The simulated air-sea CO<sub>2</sub> flux is affected by multiple physical atmospheric variables since the gas transfer velocity is often parameterized as a quadratic function of wind speed and  $f\text{CO}_{2\text{atm}}$  depends in part on atmospheric pressure and vapor pressure. GOBMs are typically forced by atmospheric reanalyses having hourly to 6-hourly timesteps. Nonetheless, simulated ocean uptake of anthropogenic carbon in GOBMs is only weakly sensitive to uncertainties in the gas transfer velocity. For example, a doubling of the gas transfer velocity led to only a 9 % increase in simulated ocean uptake of anthropogenic carbon (Sarmiento et al., 1992). The extra CO<sub>2</sub> added to the ocean from enhanced gas exchange is not transported away from the surface quickly enough, thus increasing the simulated  $f\text{CO}_{2\text{sea}}$  and reducing the change in the air-sea flux, a key feedback inherent not only in models but also in the real ocean. While models have their own problems, such as biases in simulated circulation fields, they are insensitive to the magnitude of the gas transfer velocity.

The second approach uses observation-based products for  $f\text{CO}_{2\text{sea}}$  rather than modeled fields. These data products rely on millions of in situ measurements of  $f\text{CO}_{2\text{sea}}$  archived in the Surface Ocean CO<sub>2</sub> Atlas (SOCAT, Bakker et al., 2016). Many groups have used this unevenly spaced data to produce evenly spaced gridded data products, mapping it typically to a  $1^\circ \times 1^\circ$  grid with monthly resolution and filling missing grid cells based on a series of global predictors, e.g., sea surface temperature and mixed-layer depth, obtained from satellite products and atmospheric and oceanic reanalyses (Landschützer et al., 2016; Rödenbeck et al., 2022; Chau et al., 2024; Watson et al., 2020; Zeng et al., 2022; Iida et al., 2021; Gregor et al., 2024; Gloege et al., 2022; Gregor et al., 2019). Using observed rather than simulated  $f\text{CO}_{2\text{sea}}$  is an advantage since it reflects the real ocean's air-sea interaction. But it comes with a disadvantage: the data-based approach cannot benefit from the previously mentioned feedback between the flux and  $f\text{CO}_{2\text{sea}}$ . Thus, compared to the GOBMs, data-based estimates of air-sea CO<sub>2</sub> fluxes are more sensitive to errors in the bulk flux parameterization, with associated uncertainties scaling proportionally to the imposed gas transfer velocity (Gloege and Eisaman, 2025; Jersild and Landschützer, 2024).

It is estimated that the ensemble mean  $1\sigma$  uncertainty for the 10 models is  $0.5 \text{ Pg C yr}^{-1}$  while that for the 8 data products is  $0.6\text{--}0.7 \text{ Pg C yr}^{-1}$  considering both random and systematic uncertainties (Friedlingstein et al., 2025; Ford et al., 2024). Moreover, there is a systematic discrepancy between the two approaches, where the average sink from data-based

products is  $0.5 \text{ Pg C yr}^{-1}$  larger than that from GOBMs. Friedlingstein et al. (2025) suggest a possible 10 %–20 % underestimate from the GOBMs for the ocean uptake of anthropogenic carbon owing to several potential problems: an overestimated Revelle factor, salinity biases in the Southern Ocean, an underestimated penetration of carbon into the ocean interior from weak vertical mixing and transport, and a delayed beginning for the anthropogenic perturbation, after the actual start of the industrial era (see Bronselaer et al., 2017; Terhaar et al., 2022, 2024).

Other potential sources of model-data discrepancy come from the data-based approach. First, there is the  $0.65 \pm 0.15 \text{ Pg C yr}^{-1}$  that must be added to the data-based estimates to back calculate the anthropogenic carbon flux from the total flux by removing the global effect of the net preindustrial outgassing driven by the natural imbalance between riverine input and sediment loss of carbon (Aumont et al., 2001; Regnier et al., 2022), as discussed by DeVries et al. (2023), Pérez et al. (2024) and Planchat et al. (2025). Another important source of uncertainty is the sparsity of SOCAT measurements in some key regions such as the Southern Ocean (Hauck et al., 2020, 2023; Ford et al., 2024). Finally, discrepancies may also stem from the very different temporal resolutions of the two approaches. While GOBMs compute air-sea CO<sub>2</sub> fluxes with a time step on the order of an hour, the data-based products used in GCB 2024 generally rely on monthly averaged variables. Fortunately, the data-based products do account for the effect of submonthly wind-speed variance by using monthly means of the square of observed 1- to 6-hourly wind speed when computing the gas transfer velocity. But they neglect nonlinearities stemming from submonthly variability of other physical drivers, including atmospheric pressure, sea surface temperature, and sea surface salinity.

To address this limitation, Gregor et al. (2024) developed a higher-frequency data product computing the CO<sub>2</sub> flux with 8 d temporal resolution, but they also showed its use had minimal effect on the resulting global sink estimate. Unfortunately, an 8 d frequency still does not resolve intense meteorological events, such as tropical cyclones and extratropical storms, which drive variations in atmospheric and oceanic variables on shorter time scales. Previous case studies have shown that tropical cyclones can cause substantial regional ocean carbon uptake (Gregor et al., 2024) or outgassing (Bates et al., 1998; Huang and Imberger, 2010), depending largely on the initial sign of the CO<sub>2</sub> fugacity difference at the air-sea interface. Yet the resulting global contribution of tropical cyclones to the ocean carbon sink is negligible (Lévy et al., 2012) because they mostly occur in regions with weak air-sea differences in  $f\text{CO}_2$  and because they increase CO<sub>2</sub> fluxes both into and out of the ocean, nearly canceling one another. Extratropical studies with data from floats and gliders indicate that storms in the Southern Ocean can provoke outgassing anomalies over 1–3 d, driven by concomitant variations in wind speed, atmospheric pressure, and

DIC concentrations (Carranza et al., 2024; Nicholson et al., 2022). The Argo float-based estimates suggest that Southern Ocean storms may reduce the global carbon sink by up to  $0.057 \text{ Pg C yr}^{-1}$  (Carranza et al., 2024). But storms represent only a part of the submonthly phenomena. It remains uncertain how high-frequency variability, if it were properly accounted for in data-based approaches, would affect resulting estimates of the air-sea  $\text{CO}_2$  flux at the global scale.

Although submonthly and particularly synoptic variability of ocean biogeochemical variables ( $f\text{CO}_2$ , DIC ...) cannot yet be constrained at the global scale due to the scarcity of observations, such is not the case for physical variables including not only wind speed but also atmospheric pressure, sea surface temperature and salinity. Here we ask how much this submonthly variability might affect observation-based estimates of the global ocean carbon sink, particularly in mid-latitudes where storms induce outgassing through simultaneous decreases in atmospheric pressure and increases in wind speed. Our aim is to quantify the importance of this effect, identifying the responsible non-linearities between variables and the regions where they dominate.

## 2 Methods

### 2.1 $\text{CO}_2$ flux calculations

Consistent with the GCB, our data-based air-sea  $\text{CO}_2$  flux  $F$  is computed as

$$F = k_{660}(u)A(T, S)(f\text{CO}_{2\text{atm}} - f\text{CO}_{2\text{sea}}). \quad (1)$$

where  $k_{660}$  is the gas transfer (piston) velocity at  $20^\circ\text{C}$ ,  $f\text{CO}_{2\text{atm}}$  and  $f\text{CO}_{2\text{sea}}$  are the fugacities of  $\text{CO}_2$  in the atmosphere and the ocean, and  $A = K_0(T, S) \left( \frac{Sc(T)}{660} \right)^{-\frac{1}{2}}$  with  $K_0$  being the solubility of  $\text{CO}_2$  in seawater computed from the sea surface temperature ( $T$ ) and salinity ( $S$ ) (Weiss, 1974), and the Schmidt number ( $Sc$ ) ratio is used to adjust the wind-speed formulation for gases other than  $\text{CO}_2$  and for temperatures other than  $20^\circ\text{C}$  (Wanninkhof, 2014). Positive fluxes indicate an air-to-sea  $\text{CO}_2$  flux. The  $k_{660}$  is calculated using a quadratic function of wind speed  $k_{660} = au^2$  (Wanninkhof, 1992), where  $u$  is the wind speed at 10 m. As for  $a$ , it is an empirical scaling constant adjusted for each wind dataset so that the corresponding global value of  $k$  (i.e.,  $k_{660}$  normalized to different temperatures with the Schmidt number ratio above) averages  $16.5 \text{ cm h}^{-1}$  over the ice-free ocean as derived from the observed global bomb  $^{14}\text{C}$  inventory (Naegler, 2009). Since it is based on the real ocean inventory of bomb  $^{14}\text{C}$ , this scaling approach should inherently account for the effects of submonthly variability of all variables that affect the gas transfer velocity; however there is a 20 % uncertainty associated with the bomb  $^{14}\text{C}$  inventory and thus  $k$ .

The  $\text{CO}_2$  fugacity in the atmosphere,  $f\text{CO}_{2\text{atm}}$ , is the partial pressure of  $\text{CO}_2$  corrected for the non-ideal behaviour

of the gas. The  $f\text{CO}_{2\text{atm}}$ , (in  $\mu\text{atm}$ ) is computed from the dry-air mixing ratio (or mole fraction) of  $\text{CO}_2$  (in ppm), as follows

$$f\text{CO}_{2\text{atm}} = \phi_{\text{CO}_2}(P_{\text{atm}}, T) X_{\text{CO}_2}(P_{\text{atm}} - P_{\text{vap}}(T, S)) \quad (2)$$

where  $\phi_{\text{CO}_2}$  is the fugacity coefficient from Weiss (1974),  $X_{\text{CO}_2}$  is the  $\text{CO}_2$  mole fraction in dry air (ppm),  $P_{\text{atm}}$  is the surface atmospheric pressure (atm), and  $P_{\text{vap}}$  is the partial pressure of water vapor (atm) from Weiss and Price (1980), an empirical function of  $T$  and  $S$  assuming that the air is fully saturated (100 % humidity) just above the air-sea interface.

For simplicity, in contrast with GCB data-based product, our oceanic fugacity  $f\text{CO}_{2\text{sea}}$  is not from an ocean  $f\text{CO}_2$  observation product but is instead computed from gridded products of  $T$ ,  $S$ , DIC, Alk, and total inorganic phosphorus and silicon concentrations ([P] and [Si]) using mocsy (Orr and Epitalon, 2015). This simplification enables us to evaluate the impact of submonthly variability of  $T$  and  $S$  on  $f\text{CO}_{2\text{sea}}$  while maintaining the basic GCB data-based approach.

We use hourly fields of wind speed  $u$  and surface pressure  $P_{\text{atm}}$ , and daily fields of sea surface temperature  $T$  and sea ice concentration from the fifth generation ECMWF re-analysis (ERA5, Hersbach et al., 2020) at  $0.25^\circ \times 0.25^\circ$  spatial resolution. In the gas transfer velocity formulation, the empirical scaling constant  $a$  is taken to be 0.271 as computed for the ERA5 wind speed field by Fay et al. (2021). We also use the bulk daily sea surface temperature rather than the hourly sea-surface skin temperature to be consistent with current GCB data-based estimates. All but one of those estimates use bulk sea surface temperature. Thus, we do not include effects of diurnal warming and cool skin that have been addressed in previous studies (Watson et al., 2020; Dong et al., 2022; Bellenger et al., 2023). Sea-surface salinity  $S$  is taken from the Multi Observation Global Ocean Sea Surface Salinity and Sea Surface Density dataset (Droghei et al., 2018) with  $0.25^\circ \times 0.25^\circ$  spatial resolution and 8 d temporal resolution. Atmospheric  $\text{CO}_2$  dry air mole fraction  $X_{\text{CO}_2}$  is from the NOAA Greenhouse Gas Marine Boundary Layer Reference (Lan et al., 2023), provided as  $4.5^\circ$  latitudinal bands at a temporal resolution of  $\sim 8$  d. For  $X_{\text{CO}_2}$ , we computed its monthly means because of the limited observational network used to produce this global data set, thus leaving the impact of its submonthly variability for future studies. Fields of DIC and Alk are from OceanSODA-ETHZ (Gregor and Gruber, 2021), which has  $1^\circ \times 1^\circ$  spatial resolution and monthly temporal resolution. Fields of [P] and [Si] are from a monthly climatology (Broullón et al., 2019a) derived from the 2013 World Ocean Atlas dataset (Boyer et al., 2013), also on a  $1^\circ \times 1^\circ$  grid. Before computing fluxes, all datasets are regridded to a common  $0.25^\circ \times 0.25^\circ$  grid using bilinear interpolation. Air-sea  $\text{CO}_2$  fluxes are calculated from 2009 to 2018 and, for simplicity, only for latitudes between  $60^\circ\text{S}$  and  $60^\circ\text{N}$ , thus avoiding most sea-ice covered areas. Calculations consider only the time steps when grid

cells have no ice cover. Regions poleward of 60° contribute only marginally to the global sink (Takahashi et al., 2009). Table 1 summarizes the data used in this study.

To study the sensitivity of the global ocean carbon sink to the submonthly variability that is neglected in GCB data-based products, we computed two estimates: (1) our reference, using monthly averages for all variables except for wind speed, which as in GCB already accounts for submonthly wind speed variance; and (2) our test case, using instead higher temporal resolution data for atmospheric pressure, sea-surface temperature, and sea surface salinity. Consistent with the temporal resolution of GCB 2024 data products, the reference flux  $F_{\text{ref}}$  is calculated using the monthly mean of the squared wind speed computed from hourly data of  $u^2$  and monthly means of the other variables:

$$F_{\text{ref}} = a \cdot \overline{u^2} \cdot A(\overline{T}, \overline{S}) \cdot \Delta f\text{CO}_2 \left( \overline{P_{\text{atm}}}, \overline{T}, \overline{S}, \overline{X_{\text{CO}_2}}, \overline{\text{DIC}}, \overline{\text{Alk}}, \overline{[\text{P}]^c}, \overline{[\text{Si}]^c} \right) \quad (3)$$

The overbar denotes a monthly mean, while the appended c superscript indicates a climatological monthly mean. The high-frequency flux  $F_{\text{h}}$  is calculated hourly using each variable at its highest available temporal resolution (hourly  $u$  and  $P_{\text{atm}}$ , daily  $T$ , 8-daily  $S$ , and monthly for all others). We compare  $F_{\text{ref}}$  to  $\overline{F_{\text{h}}}$ , the monthly mean of  $F_{\text{h}}$ :

$$\overline{F_{\text{h}}} = a \cdot \overline{u^2} \cdot A(\overline{T}, \overline{S}) \cdot \overline{\Delta f\text{CO}_2 \left( P_{\text{atm}}, T, S, X_{\text{CO}_2}, \text{DIC}, \text{Alk}, [\text{P}]^c, [\text{Si}]^c \right)} \quad (4)$$

To further assess the causes of differences, we also compare  $F_{\text{ref}}$  and  $\overline{F_{\text{h}}}$  to the monthly averages of two intermediate air-sea  $\text{CO}_2$  fluxes: (1)  $\overline{F_P}$  which is computed like  $\overline{F_{\text{h}}}$  but using hourly  $P$  and monthly  $T$  and  $S$  and (2)  $\overline{F_{P,T}}$ , which is computed using hourly  $P_{\text{atm}}$ , daily  $T$ , and monthly  $S$ . Then the difference  $\overline{F_P} - F_{\text{ref}}$  shows the importance of taking into account high-frequency variability of  $P_{\text{atm}}$ . Another difference  $\overline{F_{P,T}} - \overline{F_P}$  reflects the importance of taking into account daily  $T$ , while  $\overline{F_{\text{h}}} - \overline{F_{P,T}}$  shows the impact of submonthly variations of  $S$ .

Finally, the corresponding global ocean sinks of anthropogenic carbon  $S_{\text{h}}$  and  $S_{\text{ref}}$  are obtained by spatially integrating the air-sea  $\text{CO}_2$  flux (between 60° S and 60° N) and correcting for preindustrial outgassing by subtracting the global  $S_{\text{river}} = 0.65 \pm 0.15 \text{ Pg C yr}^{-1}$  (Regnier et al., 2022).

We consider that the differences  $\overline{F_{\text{h}}} - F_{\text{ref}}$  and  $S_{\text{h}} - S_{\text{ref}}$  are statistically significant only if they differ from 0 at the 99 % level using Student's  $t$ -test.

## 2.2 Reynolds decomposition

To investigate the non-linearities between high-frequency variations of the variables that are responsible for differences between  $F_{\text{ref}}$  and  $\overline{F_{\text{h}}}$ , a Reynolds decomposition is used with respect to  $u$  and  $\Delta = f\text{CO}_{2\text{atm}} - f\text{CO}_{2\text{sea}}$  for each month

from 2009 to 2018, assuming that the solubility and Schmidt number variations cancel out to give  $A = \overline{A}$  (Etcheto et Merlivat, 1988), an assumption good to within 5 % locally (Waninkhof, 2014):

$$F_{\text{h}} = aA\overline{u^2}\overline{\Delta} + aA(u')^2\overline{\Delta} + 2aA\overline{u}u'\overline{\Delta}' + aA(u')^2\overline{\Delta}' + aA\overline{u^2}\overline{\Delta}' + 2aA\overline{u}u'\overline{\Delta}' \quad (5)$$

whose monthly mean is

$$\overline{F_{\text{h}}} = \underbrace{a\overline{A\overline{u^2}\overline{\Delta}}}_{\text{bulk term}} + \underbrace{a\overline{A(u')^2\overline{\Delta}}}_{\text{variance}} + \underbrace{2a\overline{A\overline{u}u'\overline{\Delta}'}}_{\text{covariance}} + \underbrace{a\overline{A(u')^2\overline{\Delta}'}}_{\text{3rd order moment}} \quad (6)$$

The combination of the first term (mean bulk) and 2nd term (variance) is referred to as the bulk term ( $a\overline{Au^2\overline{\Delta}} = a\overline{Au^2}\overline{\Delta} + a\overline{A(u')^2\overline{\Delta}}$ ). Thus by definition it includes the enhancement from wind speed variance. The bulk term is very close to the reference flux  $F_{\text{ref}}$ . This agreement along with the assumption that  $A = \overline{A}$  is illustrated by the mean difference between  $F_{\text{ref}}$  and the bulk term ( $a\overline{Au^2\overline{\Delta}}$ ), which ranges from 0 to  $-0.2 \text{ g C m}^{-2} \text{ yr}^{-1}$  (Fig. S1), an order of magnitude smaller than the mean differences between  $\overline{F_{\text{h}}}$  and  $F_{\text{ref}}$  (Fig. 1c). This bulk term (mean bulk and variance in Eq. 6) is the same as the GCB flux definition. The GCB and other data-based reconstructions do not take into account the final two terms of Eq. (6), the correction terms. The first of those ( $u$  and  $\Delta$  covariance term) accounts for how the flux is affected by covariation between wind speed anomalies and  $\Delta$  anomalies (2nd-order moment). The second of the correction terms (3rd-order mixed moment) accounts for nonlinear interactions between wind speed variance and  $\Delta$  anomalies, thus capturing effects from skewness or asymmetry in fluctuations.

## 3 Results

### 3.1 Global ocean carbon sink sensitivity to submonthly variability

Our estimate  $S_{\text{ref}}$  is comparable in magnitude to the average from the GCB data products although it does not capture the precise interannual evolution, in particular after 2016 (Fig. 1a). This difference stems from the latest version of the DIC and Alk OceanSODA-ETHZ dataset (v2021, Gregor and Gruber, 2021), which does not capture the change in Alk, DIC and  $f\text{CO}_{2\text{sea}}$  associated with the slowdown in ocean sink after 2016 (e.g. Friedlingstein et al., 2022). This slowdown indeed only emerged in GCB data-based products after GCB 2023 (e.g. Friedlingstein et al., 2025). Both our  $S_{\text{ref}}$  and GCB account for submonthly variability of  $u$ . Our sink estimate  $S_{\text{h}}$  also accounts for submonthly variability of  $P_{\text{atm}}$ ,  $T$ , and  $S$ , and it is  $0.12 \text{ Pg C yr}^{-1}$  lower than  $S_{\text{ref}}$ . Therefore,

**Table 1.** Sources of all datasets used in this study.

Variable	Description	Time resolution	Source
$P_{\text{atm}}$	Surface pressure	Hourly	ERA5
$u$	5m wind speed	Hourly	ERA5
Sea ice	Sea ice fraction	Hourly	ERA5
$T$	Sea surface temperature	Daily	ERA5
$S$	Sea surface salinity	8-days	Droghei et al. (2018)
DIC	Dissolved inorganic carbon	Monthly	OceanSODA-ETHZ
Alk	Alkalinity	Monthly	OceanSODA-ETHZ
$X_{\text{CO}_2}$	CO <sub>2</sub> dry air mole fraction	Monthly	NOAA MBL
[P]	Phosphate concentration	Monthly climatology	Broullón et al. (2019a)
[Si]	Silicate concentration	Monthly climatology	Broullón et al. (2019a)

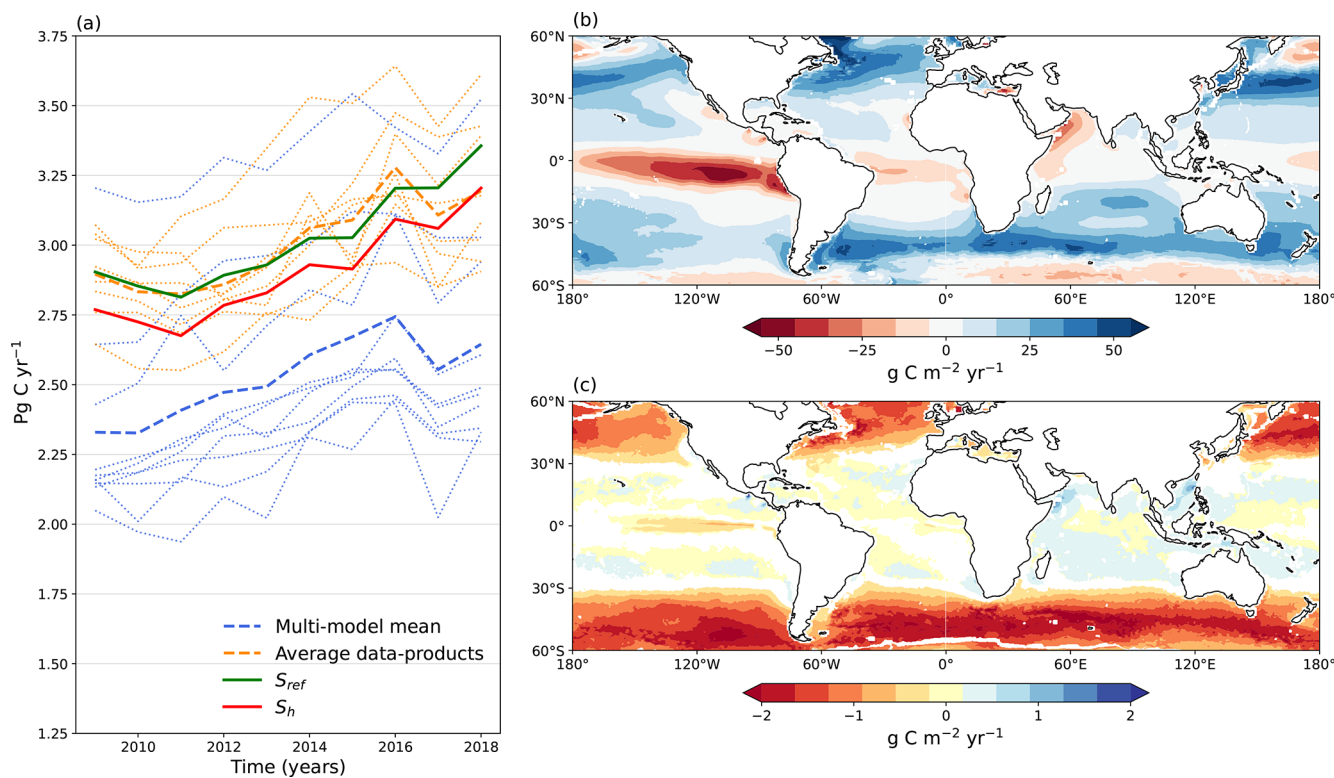


**Figure 1.** (a) Time series of the global (60° N–60° S) annual mean CO<sub>2</sub> sink (Pg C yr<sup>-1</sup>) computed from  $S_{\text{ref}}$  (thick green line),  $S_{\text{h}}$  (thick red line), and the global annual mean from the GCB 2024 data products (thin orange lines) and their mean (thick dashed orange line) as well as the GCB 2024 models (thin blue lines) and their mean (thick dashed blue line). Also shown are maps for the 2009–2018 mean of (b) the air-sea CO<sub>2</sub> reference flux  $F_{\text{ref}}$  and (c) the difference between the monthly mean of the high frequency flux  $\overline{F}_{\text{h}}$  and  $F_{\text{ref}}$ , where positive values indicate less outgassing or more uptake with  $\overline{F}_{\text{h}}$  than with  $F_{\text{ref}}$ .

the standard approach, which neglects all submonthly variability besides that of  $u$ , overestimates the carbon sink by 0.12 Pg C yr<sup>-1</sup>. On average between 2009 and 2018, this difference corresponds to 5 % of the carbon sink  $S_{\text{ref}}$  but 25 % of the discrepancy between models and data products from GCB ( $\sim 0.5$  Pg C yr<sup>-1</sup>). Our computed difference does not change over 2009 to 2018 and remains statistically significant.

The spatial distribution of  $F_{\text{ref}}$  (Fig. 1b) is consistent with the fluxes from the SeaFlux product (Fay et al., 2021, Fig. S2). The 2009–2018 mean difference  $\overline{F}_{\text{h}} - F_{\text{ref}}$  shows that the discrepancy between the two fluxes stems largely from latitudes between 30 and 60° in both hemispheres (Fig. 1c). In these regions relative to  $F_{\text{ref}}$ ,  $\overline{F}_{\text{h}}$  exhibits either more outgassing (North Atlantic, Southern Ocean) or less uptake (North Pacific, by 1.5 g C m<sup>-2</sup> yr<sup>-1</sup> on average). A weaker opposing effect is seen in tropics, where sinks

are increased by  $0.5 \text{ g C m}^{-2} \text{ yr}^{-1}$  on average, and by up to  $1 \text{ g C m}^{-2} \text{ yr}^{-1}$  in the Arabian Sea and South China Sea.

Differences in the mid-latitudes are mainly due to atmospheric pressure variations, whereas differences in the tropics are driven by sea surface temperature variations. The former can be seen in the  $\overline{F_P} - F_{\text{ref}}$  map (Fig. 2a) and the  $\overline{F_{P,T}} - \overline{F_P}$  map (Fig. 2b). Atmospheric pressure variations reduce the carbon sink estimate by  $0.136 \text{ Pg C yr}^{-1}$  on average, an effect that is slightly weakened by sea surface temperature variations which increase the sink by  $0.016 \text{ Pg C yr}^{-1}$ . On synoptic timescales (2–10 d), low pressure perturbations are associated with stronger winds, so periods of strong  $\text{CO}_2$  exchange have lower atmospheric pressure and thus lower atmospheric  $\text{CO}_2$  fugacity. Thus wind speed and atmospheric pressure covariance leads to an anomalous outgassing correction term in the midlatitudes. Further separation of  $\overline{F_{P,T}} - \overline{F_P}$  into atmospheric and oceanic components (Fig. S3b) reveal that temperature variations mainly affect ocean  $f\text{CO}_{2\text{sea}}$ , but have negligible effect on vapor pressure. The anomalous ingassing in the Arabian Sea appears to result from an increase in submonthly variability of wind speed, which drives stronger upwelling and hence surface cooling, thus reducing  $f\text{CO}_{2\text{sea}}$ . The remaining effect of salinity ( $\overline{F_h} - \overline{F_{P,T}}$ ) is negligible.

### 3.2 Relative importance of the correction terms

The relative importance of the different terms is diagnosed by the Reynolds decomposition in Eq. (6). The wind speed variance term, which is already accounted for in the GCB data-based products, is the dominant source of submonthly nonlinearity (Fig. 3a). It results in an increase in the estimated  $60^\circ\text{N}$ – $60^\circ\text{S}$  ocean carbon sink by  $0.36 \text{ Pg C yr}^{-1}$ . This increase is situated mainly in the mid-latitudes, peaking at  $40^\circ\text{S}$  and  $40^\circ\text{N}$  (Figs. 3, S4).

Our first correction term (covariance) accounts for 90 % of the correction, whereas the third-order moment is weaker. Together they result in a global outgassing anomaly whose magnitude is one-third of the wind variance term and opposite in sign. About 85 % of this contribution is situated between  $60$ – $30^\circ\text{S}$  and amounts to a reduction of  $0.1 \text{ Pg C yr}^{-1}$  (Fig. 3a). The other main region where the correction terms reduce the sink is between  $30$ – $60^\circ\text{N}$ , but that reduction of  $0.03 \text{ Pg C yr}^{-1}$  is largely offset by the  $0.026 \text{ Pg C yr}^{-1}$  increase between  $30^\circ\text{S}$ – $30^\circ\text{N}$ . Although the covariance term is generally weaker than the wind speed variance term, it has a similar magnitude in the tropics and dominates south of  $50^\circ\text{S}$  (Fig. 3b).

## 4 Discussion

This study reveals that accounting for hourly variability in atmospheric pressure and including the small compensation from daily variability in sea surface temperature, reduces data-based estimates of the global ocean carbon sink

by  $0.12 \text{ Pg C yr}^{-1}$ , thereby closing 25 % of the gap between those data products and the GOBMs. While the 8 d product from Gregor et al. (2024) offers higher frequency atmospheric and oceanic  $\text{CO}_2$  fugacities than the standard monthly products used in the GCB data-based ocean flux estimates, the resulting computed global flux is essentially unchanged. Thus, it appears that at least synoptic frequency is needed to adequately capture the effect of atmospheric variability. Whether or not 6-hourly or daily atmospheric pressure data would be sufficient in place of our use of hourly data remains a question for future research.

The Reynolds decomposition of the high-resolution  $\text{CO}_2$  flux confirms that the submonthly variation in wind speed, already accounted for in the ocean data products, is the most important nonlinearity. It generally increases sink estimates outside the tropics with peaks at  $40^\circ\text{S}$  and  $40^\circ\text{N}$ . Conversely, our correction due to the submonthly covariance of wind speed and atmospheric pressure leads to outgassing anomalies in the midlatitudes. The reason is that midlatitude synoptic disturbances have strong winds that favor air-sea exchange but also reduce atmospheric pressure, thus lowering atmospheric  $\text{CO}_2$  fugacity, which favors outgassing. This correction is particularly large in waters south of  $30^\circ\text{S}$ , representing 85 % of its impact on the global ocean carbon sink. South of  $50^\circ\text{S}$ , it becomes the main source of nonlinearity.

While the nonlinearities underlined here appear to explain 25 % of the average gap between models and data-based products, their effect seems constant in time. Therefore, they do not seem to explain the temporal evolution of the gap underlined by Friedlingstein et al. (2025). The exact correction will depend on the calculation details and thus will differ between data-based products. For future GCB exercises, we suggest that each group compute independently both directions of the flux  $k_{660}(u)A(T, S)f\text{CO}_{2\text{atm}}$  and  $k_{660}(u)A(T, S)f\text{CO}_{2\text{sea}}$  at maximum temporal resolution before computing monthly averages and taking the difference to obtain the flux. We also leave for future studies the question of whether or not accounting for submonthly variations in atmospheric  $X_{\text{CO}_2}$ , particularly those due to covariations with  $P_{\text{atm}}$ , may substantially alter data-based estimates of ocean carbon uptake. The gap between data-based products and GOBMs also depends on model resolution and their representation of coastal regions (e.g. Resplandy et al., 2024) as well as on processes not yet commonly included in the flux parameterization, such as the ocean cool skin ( $+0.3 \text{ Pg C yr}^{-1}$ , Dong et al., 2022), rain ( $+0.14$ – $0.19 \text{ Pg C yr}^{-1}$ , Parc et al., 2024) and wave breaking-induced bubbles. While these bubbles may increase modeled  $\text{CO}_2$  uptake by only  $0.07 \text{ Pg C yr}^{-1}$  (Rustogi et al., 2025), they could increase data-based estimates by up to  $0.3$ – $0.4 \text{ Pg C yr}^{-1}$  (Dong et al., 2025). Similarly, Bellenger et al. (2023) showed that the cool skin temperature effect is three times smaller in a model framework because of the feedback process mentioned earlier and because gas exchange is not rate limiting, unlike carbon transfer to the ocean interior. Including

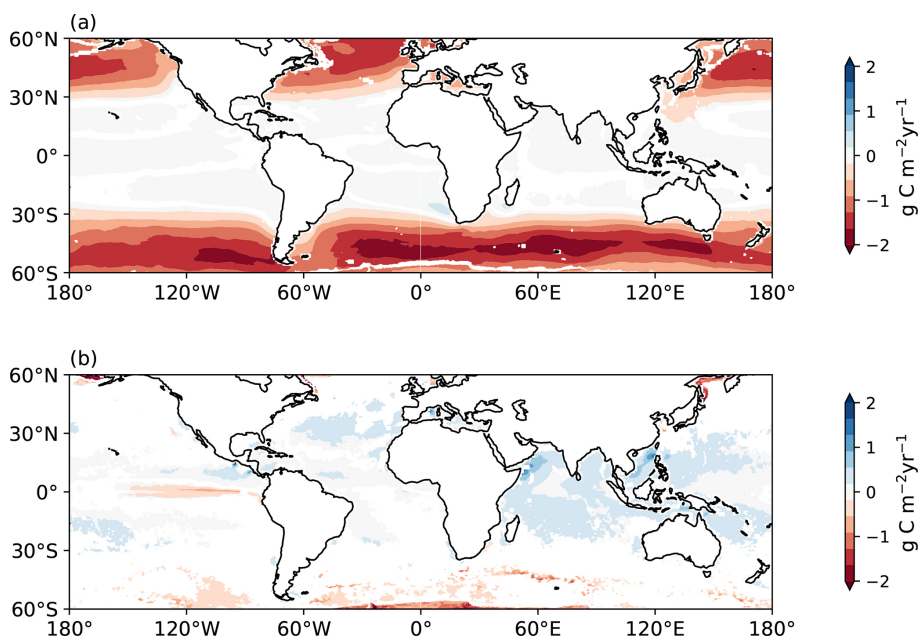


**Figure 2.** Maps averaged over 2009–2018 for effects on observation-based air-sea CO<sub>2</sub> fluxes from (a) submonthly variability of atmospheric pressure ( $F_P - F_{ref}$ ) and (b) submonthly variability of temperature ( $F_{P,T} - F_P$ ).

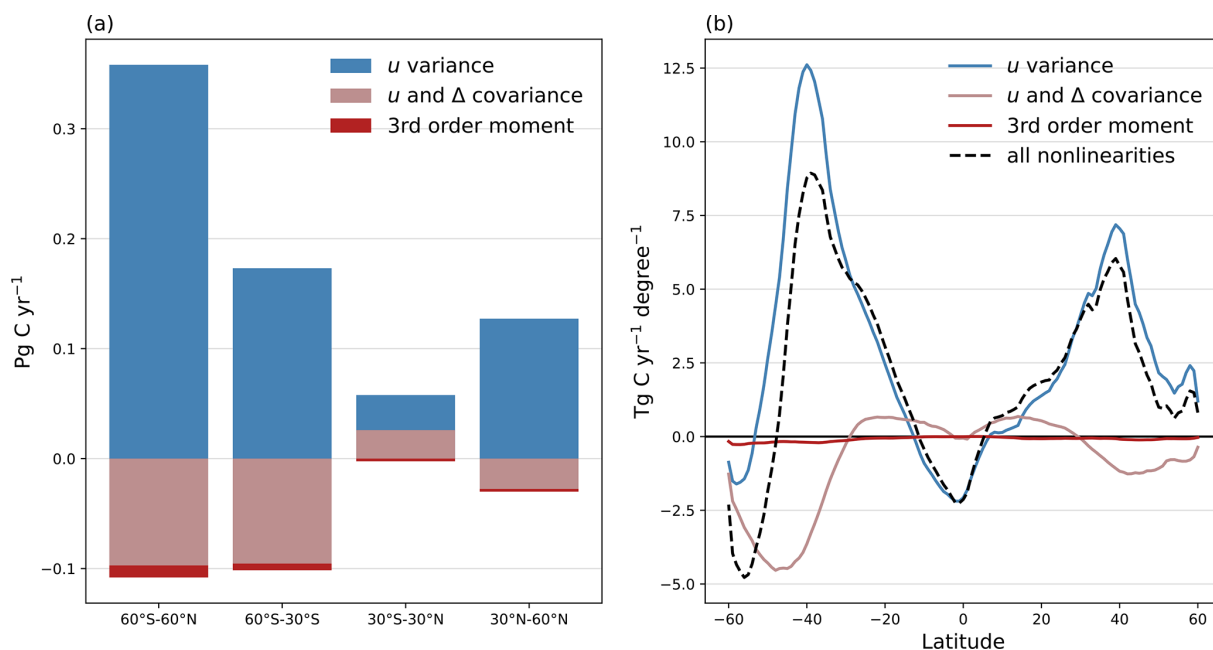


**Figure 3.** (a) Contribution of the final 3 terms in Eq. (6) to ocean carbon uptake in different latitudinal bands. (b) Zonal integral of the final three terms in Eq. (6) (blue, pink and red lines) and their sum (dashed black line).

the cool skin effect in both data-based products and GOBMs could thus increase the gap by about +0.2 Pg C yr<sup>-1</sup>. The addition of new processes in the calculation of carbon fluxes may further increase the gap between estimates from data-based products versus GOBMs.

Our results suggest that the previous estimate of the storm-induced outgassing for the Southern Ocean of 0.057 Pg C yr<sup>-1</sup> (Carranza et al., 2024) is only a fraction of the total effect of submonthly variability on the ocean sink in this region. Indeed, we found a mean outgassing of about 0.1 Pg C yr<sup>-1</sup> in the 60–30°S band mainly driven by atmo-

spheric pressure and wind speed covariance. On the other hand, previous observations in the Southern Ocean from Argo floats (Carranza et al., 2024) and gliders (Nicholson et al., 2022) suggest that submonthly variability of ocean biogeochemical variables have a major impact on storm induced outgassing. Those observations suggest that entrainment of cold, DIC-rich subsurface water into the surface mixed layer is the leading cause of mean storm-driven CO<sub>2</sub> outgassing in the Southern Ocean (Carranza et al., 2024). Monthly  $f\text{CO}_2$ -products cannot resolve storm induced  $f\text{CO}_{2\text{sea}}$ , while GOBMs may underestimate storm-driven vertical transport of DIC (Carranza et al., 2024). Therefore, submonthly variability of biogeochemical variables in the Southern Ocean demands more attention, both for data- and model-based estimates. While our study helps to narrow the data-model gap, its continued growth and the large disparities among data-based products and among models underscore the need for further advances to constrain ocean carbon uptake, advances that are also key to reducing, by difference, much larger uncertainties associated with the terrestrial biosphere.

**Data availability.** Estimates of the CO<sub>2</sub> fluxes for the different diagnostics made here are publicly available at the Zenodo repository <https://doi.org/10.5281/zenodo.15848192> (Dombret et al., 2025). ERA5 reanalysis data from the ECMWF (Hersbach et al., 2020) was obtained through the Copernicus Climate Change Service (Hersbach et al., 2023) (<https://doi.org/10.24381/cds.adbb2d47>). The results contain modified Copernicus Climate Change Service information 2020. Neither the European Commission nor ECMWF is responsible for any use that may be made of the Copernicus information or data it contains. The CO<sub>2</sub> dry air mole fraction data are from the NOAA Greenhouse Gas Marine Boundary Layer Reference (<https://gml.noaa.gov/ccgg/mbldata.php>, last access: 22 March 2023). The sea surface salinity values were downloaded from EU Copernicus Marine Service Information (<https://doi.org/10.48670/moi-00051>, CMEMS, 2023). Global DIC and Alk bulk values are from the OceanSODA–ETHZ climatology dataset (<https://doi.org/10.25921/m5wx-ja34>, Gregor and Gruber, 2020). The Broullón et al. (2019a) monthly climatologies of dissolved inorganic silicon and phosphorus are available at <https://doi.org/10.20350/digitalCSIC/8644> (Broullón et al., 2019b).

**Supplement.** The supplement related to this article is available online at <https://doi.org/10.5194/bg-23-4133-2026-supplement>.

**Author contributions.** Conceptualization JD, HB, XP, JCO; Methodology: LP, XP, JCO, Formal analysis: JD, XP, HB; Visualization: JD; Writing: JD, HB, JCO, LK, FC, LB, MG, RS, SB.

**Competing interests.** The contact author has declared that none of the authors has any competing interests.

**Disclaimer.** Publisher's note: Copernicus Publications remains neutral with regard to jurisdictional claims made in the text, published maps, institutional affiliations, or any other geographical representation in this paper. The authors bear the ultimate responsibility for providing appropriate place names. Views expressed in the text are those of the authors and do not necessarily reflect the views of the publisher.

**Acknowledgements.** This study used the EU Copernicus Marine Service Information; <https://doi.org/10.48670/moi-00051> (CMEMS, 2023). To process the data, this study benefited from the IPSL mesocenter ESPRI facility which is supported by CNRS, UPMC, Labex L-IPSL, CNES and Ecole Polytechnique. JCO and MG were funded by EU grant 101083922 (OceanICU).

**Financial support.** RS acknowledges funding from the EU's Horizon Europe research and innovation programme under ESM2025 (grant no. 101003536) and OptimESM (grant no. 101081193) as well as the ANR-France 2030 as part of the PEPR TRACCS programme (grant no. ANR-22-EXTR-0009).

**Review statement.** This paper was edited by Frédéric Gazeau and reviewed by Yuanxu Dong and one anonymous referee.

## References

- Aumont, O., Orr, J. C., Monfray, P., Ludwig, W., Amiotte-Suchet, P., and Probst, J.: Riverine-driven interhemispheric transport of carbon, *Global Biogeochem. Cy.*, 15, 393–405, <https://doi.org/10.1029/1999GB001238>, 2001.
- Bakker, D. C. E., Pfeil, B., Landa, C. S., Metzl, N., O'Brien, K. M., Olsen, A., Smith, K., Cosca, C., Harasawa, S., Jones, S. D., Nakaoka, S., Nojiri, Y., Schuster, U., Steinhoff, T., Sweeney, C., Takahashi, T., Tilbrook, B., Wada, C., Wanninkhof, R., Alin, S. R., Balestrini, C. F., Barbero, L., Bates, N. R., Bianchi, A. A., Bonou, F., Boutin, J., Bozec, Y., Burger, E. F., Cai, W.-J., Castle, R. D., Chen, L., Chierici, M., Currie, K., Evans, W., Featherstone, C., Feely, R. A., Fransson, A., Goyet, C., Greenwood, N., Gregor, L., Hankin, S., Hardman-Mountford, N. J., Harlay, J., Hauck, J., Hoppema, M., Humphreys, M. P., Hunt, C. W., Huss, B., Ibáñez, J. S. P., Johannessen, T., Keeling, R., Kitidis, V., Körtzinger, A., Kozyr, A., Krasakopoulou, E., Kuwata, A., Landschützer, P., Lauvset, S. K., Lefèvre, N., Lo Monaco, C., Manke, A., Mathis, J. T., Merlivat, L., Millero, F. J., Monteiro, P. M. S., Munro, D. R., Murata, A., Newberger, T., Omar, A. M., Ono, T., Paterson, K., Pearce, D., Pierrot, D., Robbins, L. L., Saito, S., Salisbury, J., Schlitzer, R., Schneider, B., Schweitzer, R., Sieger, R., Skjelvan, I., Sullivan, K. F., Sutherland, S. C., Sutton, A. J., Tadokoro, K., Telszewski, M., Tuma, M., van Heuven, S. M. A. C., Vandemark, D., Ward, B., Watson, A. J., and Xu, S.: A multi-decade record of high-quality  $f\text{CO}_2$  data in version 3 of the Surface Ocean CO<sub>2</sub> Atlas (SOCAT), *Earth Syst. Sci. Data*, 8, 383–413, <https://doi.org/10.5194/essd-8-383-2016>, 2016.

- Bates, N. R., Knap, A. H., and Michaels, A. F.: Contribution of hurricanes to local and global estimates of air–sea exchange of CO<sub>2</sub>, *Nature*, 395, 58–61, <https://doi.org/10.1038/25703>, 1998.
- Bellenger, H., Bopp, L., Ethé, C., Ho, D., Duvel, J. P., Flavoni, S., Guez, L., Kataoka, T., Perrot, X., Parc, L., and Watanabe, M.: Sensitivity of the Global Ocean Carbon Sink to the Ocean Skin in a Climate Model, *J. Geophys. Res.–Oceans*, 128, e2022JC019479, <https://doi.org/10.1029/2022JC019479>, 2023.
- Boyer, T. P., Antonov, J. I., Baranova, O. K., Coleman, C., Garcia, H. E., Grodsky, A., Johnson, D. R., Locarnini, R. A., Mishonov, A. V., O’Brien, T. D., Paver, C. R., Reagan, J. R., Seidov, D., Smolyar, I. V., and Zweng, M. M.: World Ocean Database 2013, National Oceanographic Data Center [data set], <https://doi.org/10.25607/OBP-1454>, 2013.
- Bronselaer, B., Winton, M., Russell, J., Sabine, C. L., and Khatiwala, S.: Agreement of CMIP5 Simulated and Observed Ocean Anthropogenic CO<sub>2</sub> Uptake, *Geophys. Res. Lett.*, 44, <https://doi.org/10.1002/2017GL074435>, 2017.
- Broullón, D., Pérez, F. F., Velo, A., Hoppema, M., Olsen, A., Takahashi, T., Key, R. M., Tanhua, T., González-Dávila, M., Jeansson, E., Kozyr, A., and van Heuven, S. M. A. C.: A global monthly climatology of total alkalinity: a neural network approach, *Earth Syst. Sci. Data*, 11, 1109–1127, <https://doi.org/10.5194/essd-11-1109-2019>, 2019a.
- Broullón, D., Pérez, F. F., Velo, A., Hoppema, M., Olsen, A., Takahashi, T., Key, R. M., González-Dávila, M., Tanhua, T., Jeansson, E., Kozyr, A., and Van Heuven, S.: A global monthly climatology of total alkalinity: a neural network approach (2019), Digital.CSIC [data set], <https://doi.org/10.20350/digitalCSIC/8644>, 2019b.
- Carranza, M. M., Long, Matthew C., Di Luca, A., Fassbender, A. J., Johnson, K. S., Takeshita, Y., Mongwe, P., and Turner, K. E.: Extratropical storms induce carbon outgassing over the Southern Ocean, *npj Clim. Atmos. Sci.*, 7, 106, <https://doi.org/10.1038/s41612-024-00657-7>, 2024.
- Chau, T., Chevallier, F., and Gehlen, M.: Global Analysis of Surface Ocean CO<sub>2</sub> Fugacity and Air–Sea Fluxes With Low Latency, *Geophys. Res. Lett.*, 51, e2023GL106670, <https://doi.org/10.1029/2023GL106670>, 2024.
- DeVries, T., Yamamoto, K., Wanninkhof, R., Gruber, N., Hauck, J., Müller, J. D., Bopp, L., Carroll, D., Carter, B., Chau, T., Doney, S. C., Gehlen, M., Gloege, L., Gregor, L., Henson, S., Kim, J. H., Iida, Y., Ilyina, T., Landschützer, P., Le Quéré, C., Munro, D., Nissen, C., Patara, L., Pérez, F. F., Resplandy, L., Rodgers, K. B., Schwinger, J., Séférian, R., Sicardi, V., Terhaar, J., Triñanes, J., Tsujino, H., Watson, A., Yasunaka, S., and Zeng, J.: Magnitude, Trends, and Variability of the Global Ocean Carbon Sink From 1985 to 2018, *Global Biogeochem. Cy.*, 37, e2023GB007780, <https://doi.org/10.1029/2023GB007780>, 2023.
- Dombret, J., Bellenger, H., Perrot, X., Parc, L., bopp, . laurent ., Kwiatkowski, L., Séférian, R., Berthet, S., Gehlen, M., Chevallier, F., and Orr, J.: Data-based estimates of ocean carbon uptake biased high from neglect of submonthly atmospheric pressure variability, Zenodo [data set], <https://doi.org/10.5281/zenodo.15848192>, 2025.
- Dong, Y., Bakker, D. C. E., Bell, T. G., Huang, B., Landschützer, P., Liss, P. S., and Yang, M.: Update on the Temperature Corrections of Global Air–Sea CO<sub>2</sub> Flux Estimates, *Global Biogeochem. Cy.*, 36, e2022GB007360, <https://doi.org/10.1029/2022GB007360>, 2022.
- Dong, Y., Yang, M., Bell, T. G., Marandino, C. A., and Woolf, D. K.: Asymmetric bubble-mediated gas transfer enhances global ocean CO<sub>2</sub> uptake, *Nat. Commun.*, 16, 10595, <https://doi.org/10.1038/s41467-025-66652-5>, 2025.
- Droghei, R., Buongiorno Nardelli, B., and Santoleri, R.: A New Global Sea Surface Salinity and Density Dataset From Multivariate Observations (1993–2016), *Front. Mar. Sci.*, 5, 84, <https://doi.org/10.3389/fmars.2018.00084>, 2018.
- Etcheto, J. and Merlivat, L.: Satellite determination of the carbon dioxide exchange coefficient at the ocean–atmosphere interface: A first step, *J. Geophys. Res.*, 93, 15669–15678, <https://doi.org/10.1029/JC093iC12p15669>, 1988.
- E.U. Copernicus Marine Service Information (CMEMS): Mediterranean Sea – High Resolution Diurnal Subskin Sea Surface Temperature Analysis, Marine Data Store (MDS) [data set], <https://doi.org/10.48670/moi-00170>, 2023.
- Fay, A. R., Gregor, L., Landschützer, P., McKinley, G. A., Gruber, N., Gehlen, M., Iida, Y., Laruelle, G. G., Rödenbeck, C., Roobaert, A., and Zeng, J.: SeaFlux: harmonization of air–sea CO<sub>2</sub> fluxes from surface pCO<sub>2</sub> data products using a standardized approach, *Earth Syst. Sci. Data*, 13, 4693–4710, <https://doi.org/10.5194/essd-13-4693-2021>, 2021.
- Ford, D. J., Blannin, J., Watts, J., Watson, A. J., Landschützer, P., Jersild, A., and Shutler, J. D.: A Comprehensive Analysis of Air–Sea CO<sub>2</sub> Flux Uncertainties Constructed From Surface Ocean Data Products, *Global Biogeochem. Cy.*, 38, e2024GB008188, <https://doi.org/10.1029/2024GB008188>, 2024.
- Friedlingstein, P., Jones, M. W., O’Sullivan, M., Andrew, R. M., Bakker, D. C. E., Hauck, J., Le Quéré, C., Peters, G. P., Peters, W., Pongratz, J., Sitch, S., Canadell, J. G., Ciais, P., Jackson, R. B., Alin, S. R., Anthoni, P., Bates, N. R., Becker, M., Bellouin, N., Bopp, L., Chau, T. T. T., Chevallier, F., Chini, L. P., Cronin, M., Currie, K. I., Decharme, B., Djeutchouang, L. M., Dou, X., Evans, W., Feely, R. A., Feng, L., Gasser, T., Gilfillan, D., Gkritzalis, T., Grassi, G., Gregor, L., Gruber, N., Gürses, Ö., Harris, I., Houghton, R. A., Hurtt, G. C., Iida, Y., Ilyina, T., Luijkx, I. T., Jain, A., Jones, S. D., Kato, E., Kennedy, D., Klein Goldewijk, K., Knauer, J., Korsbakken, J. I., Körtzinger, A., Landschützer, P., Lauvset, S. K., Lefèvre, N., Lienert, S., Liu, J., Marland, G., McGuire, P. C., Melton, J. R., Munro, D. R., Nabel, J. E. M. S., Nakaoka, S.-I., Niwa, Y., Ono, T., Pierrot, D., Poulter, B., Rehder, G., Resplandy, L., Robertson, E., Rödenbeck, C., Rosan, T. M., Schwinger, J., Schwingshackl, C., Séférian, R., Sutton, A. J., Sweeney, C., Tanhua, T., Tans, P. P., Tian, H., Tilbrook, B., Tubiello, F., van der Werf, G. R., Vuichard, N., Wada, C., Wanninkhof, R., Watson, A. J., Willis, D., Wiltshire, A. J., Yuan, W., Yue, C., Yue, X., Zaehle, S., and Zeng, J.: Global Carbon Budget 2021, *Earth Syst. Sci. Data*, 14, 1917–2005, <https://doi.org/10.5194/essd-14-1917-2022>, 2022.
- Friedlingstein, P., O’Sullivan, M., Jones, M. W., Andrew, R. M., Hauck, J., Landschützer, P., Le Quéré, C., Li, H., Luijkx, I. T., Olsen, A., Peters, G. P., Peters, W., Pongratz, J., Schwingshackl, C., Sitch, S., Canadell, J. G., Ciais, P., Jackson, R. B., Alin, S. R., Arneeth, A., Arora, V., Bates, N. R., Becker, M., Bellouin, N., Berghoff, C. F., Bittig, H. C., Bopp, L., Cadule, P., Campbell, K., Chamberlain, M. A., Chandra, N., Chevallier, F., Chini, L. P., Colligan, T., Decayeux, J., Djeutchouang, L. M., Dou, X., Duran

- Rojas, C., Enyo, K., Evans, W., Fay, A. R., Feely, R. A., Ford, D. J., Foster, A., Gasser, T., Gehlen, M., Gkritzalis, T., Grassi, G., Gregor, L., Gruber, N., Gürses, Ö., Harris, I., Hefner, M., Heinke, J., Hurtt, G. C., Iida, Y., Ilyina, T., Jacobson, A. R., Jain, A. K., Jarníková, T., Jersild, A., Jiang, F., Jin, Z., Kato, E., Keeling, R. F., Klein Goldewijk, K., Knauer, J., Korsbakken, J. I., Lan, X., Lauvset, S. K., Lefèvre, N., Liu, Z., Liu, J., Ma, L., Maksyutov, S., Marland, G., Mayot, N., McGuire, P. C., Metzl, N., Monacci, N. M., Morgan, E. J., Nakaoka, S.-I., Neill, C., Niwa, Y., Nützel, T., Olivier, L., Ono, T., Palmer, P. I., Pierrot, D., Qin, Z., Resplandy, L., Roobaert, A., Rosan, T. M., Rödenbeck, C., Schwinger, J., Smallman, T. L., Smith, S. M., Sospedra-Alfonso, R., Steinhoff, T., Sun, Q., Sutton, A. J., Séférian, R., Takao, S., Tatebe, H., Tian, H., Tilbrook, B., Torres, O., Tourigny, E., Tsujino, H., Tubiello, F., van der Werf, G., Wanninkhof, R., Wang, X., Yang, D., Yang, X., Yu, Z., Yuan, W., Yue, X., Zaehle, S., Zeng, N., and Zeng, J.: Global Carbon Budget 2024, *Earth Syst. Sci. Data*, 17, 965–1039, <https://doi.org/10.5194/essd-17-965-2025>, 2025.
- Gloege, L. and Eisaman, M. D.: Regional Uncertainty Analysis in the Air–Sea CO<sub>2</sub> Flux, *Earth and Space Science*, 12, e2024EA004032, <https://doi.org/10.1029/2024EA004032>, 2025.
- Gloege, L., Yan, M., Zheng, T., and McKinley, G. A.: Improved Quantification of Ocean Carbon Uptake by Using Machine Learning to Merge Global Models and pCO<sub>2</sub> Data, *J. Adv. Model. Earth Sy.*, 14, e2021MS002620, <https://doi.org/10.1029/2021MS002620>, 2022.
- Gregor, L. and Gruber, N.: OceanSODA-ETHZ: A global gridded dataset of the surface ocean carbonate system for seasonal to decadal studies of ocean acidification (v2025) (NCEI Accession 0220059). v2.2, NOAA National Centers for Environmental Information [data set], <https://doi.org/10.25921/m5wx-ja34> (last access: 2021), 2020.
- Gregor, L. and Gruber, N.: OceanSODA-ETHZ: a global gridded data set of the surface ocean carbonate system for seasonal to decadal studies of ocean acidification, *Earth Syst. Sci. Data*, 13, 777–808, <https://doi.org/10.5194/essd-13-777-2021>, 2021.
- Gregor, L., Lebehot, A. D., Kok, S., and Scheel Monteiro, P. M.: A comparative assessment of the uncertainties of global surface ocean CO<sub>2</sub> estimates using a machine-learning ensemble (CSIR-ML6 version 2019a) – have we hit the wall?, *Geosci. Model Dev.*, 12, 5113–5136, <https://doi.org/10.5194/gmd-12-5113-2019>, 2019.
- Gregor, L., Shutler, J., and Gruber, N.: High-Resolution Variability of the Ocean Carbon Sink, *Global Biogeochem. Cy.*, 38, e2024GB008127, <https://doi.org/10.1029/2024GB008127>, 2024.
- Hauck, J., Zeising, M., Le Quéré, C., Gruber, N., Bakker, D. C. E., Bopp, L., Chau, T. T. T., Gürses, Ö., Ilyina, T., Landschützer, P., Lenton, A., Resplandy, L., Rödenbeck, C., Schwinger, J., and Séférian, R.: Consistency and Challenges in the Ocean Carbon Sink Estimate for the Global Carbon Budget, *Front. Mar. Sci.*, 7, 571720, <https://doi.org/10.3389/fmars.2020.571720>, 2020.
- Hauck, J., Nissen, C., Landschützer, P., Rödenbeck, C., Bushinsky, S., and Olsen, A.: Sparse observations induce large biases in estimates of the global ocean CO<sub>2</sub> sink: an ocean model subsampling experiment, *Phil. Trans. R. Soc. A.*, 381, 20220063, <https://doi.org/10.1098/rsta.2022.0063>, 2023.
- Hersbach, H., Bell, B., Berrisford, P., Hirahara, S., Horányi, A., Muñoz-Sabater, J., Nicolas, J., Peubey, C., Radu, R., Schepers, D., Simmons, A., Soci, C., Abdalla, S., Abellan, X., Balsamo, G., Bechtold, P., Biavati, G., Bidlot, J., Bonavita, M., De Chiara, G., Dahlgren, P., Dee, D., Diamantakis, M., Dragani, R., Flemming, J., Forbes, R., Fuentes, M., Geer, A., Haimberger, L., Healy, S., Hogan, R. J., Hólm, E., Janisková, M., Keeley, S., Laloyaux, P., Lopez, P., Lupu, C., Radnoti, G., De Rosnay, P., Rozum, I., Vamborg, F., Villaume, S., and Thépaut, J.: The ERA5 global reanalysis, *Q. J. Roy. Meteor. Soc.*, 146, 1999–2049, <https://doi.org/10.1002/qj.3803>, 2020.
- Hersbach, H., Bell, B., Berrisford, P., Biavati, G., Horányi, A., Muñoz Sabater, J., Nicolas, J., Peubey, C., Radu, R., Rozum, I., Schepers, D., Simmons, A., Soci, C., Dee, D., and Thépaut, J.-N.: ERA5 hourly data on single levels from 1940 to present, Copernicus Climate Change Service (C3S) Climate Data Store (CDS) [data set], <https://doi.org/10.24381/cds.adbb2d47>, 2023.
- Huang, P. and Imberger, J.: Variation of pCO<sub>2</sub> in ocean surface water in response to the passage of a hurricane, *J. Geophys. Res.*, 115, 2010JC006185, <https://doi.org/10.1029/2010JC006185>, 2010.
- Iida, Y., Takatani, Y., Kojima, A., and Ishii, M.: Global trends of ocean CO<sub>2</sub> sink and ocean acidification: an observation-based reconstruction of surface ocean inorganic carbon variables, *J. Oceanogr.*, 77, 323–358, <https://doi.org/10.1007/s10872-020-00571-5>, 2021.
- Jersild, A. and Landschützer, P.: A Spatially Explicit Uncertainty Analysis of the Air-Sea CO<sub>2</sub> Flux From Observations, *Geophys. Res. Lett.*, 51, e2023GL106636, <https://doi.org/10.1029/2023GL106636>, 2024.
- Lan, X., Tans, P., Thoning, K., and NOAA Global Monitoring Laboratory: NOAA Greenhouse Gas Marine Boundary Layer Reference, NOAA [data set], <https://doi.org/10.15138/DVNP-F961>, 2023.
- Landschützer, P., Gruber, N., and Bakker, D. C. E.: Decadal variations and trends of the global ocean carbon sink, *Global Biogeochem. Cy.*, 30, 1396–1417, <https://doi.org/10.1002/2015GB005359>, 2016.
- Lévy, M., Lengaigne, M., Bopp, L., Vincent, E. M., Madec, G., Ethé, C., Kumar, D., and Sarma, V. V. S. S.: Contribution of tropical cyclones to the air-sea CO<sub>2</sub> flux: A global view, *Global Biogeochem. Cy.*, 26, 2011GB004145, <https://doi.org/10.1029/2011GB004145>, 2012.
- Naegler, T.: Reconciliation of excess <sup>14</sup>C-constrained global CO<sub>2</sub> piston velocity estimates, *Tellus B*, 61, 372, <https://doi.org/10.1111/j.1600-0889.2008.00408.x>, 2009.
- Nicholson, S.-A., Whitt, D. B., Fer, I., Du Plessis, M. D., Lebéhot, A. D., Swart, S., Sutton, A. J., and Monteiro, P. M. S.: Storms drive outgassing of CO<sub>2</sub> in the subpolar Southern Ocean, *Nat. Commun.*, 13, 158, <https://doi.org/10.1038/s41467-021-27780-w>, 2022.
- Orr, J. C. and Epitalon, J.-M.: Improved routines to model the ocean carbonate system: mocsy 2.0, *Geosci. Model Dev.*, 8, 485–499, <https://doi.org/10.5194/gmd-8-485-2015>, 2015.
- Parc, L., Bellenger, H., Bopp, L., Perrot, X., and Ho, D. T.: Global ocean carbon uptake enhanced by rainfall, *Nat. Geosci.*, 17, 851–857, <https://doi.org/10.1038/s41561-024-01517-y>, 2024.
- Pérez, F. F., Becker, M., Goris, N., Gehlen, M., López-Mozos, M., Tjiputra, J., Olsen, A., Müller, J. D., Huertas, I. E., Chau, T. T. T., Cainzos, V., Velo, A., Benard, G., Hauck, J., Gruber, N., and Wanninkhof, R.: An Assessment of CO<sub>2</sub> Storage and Sea-Air

- Fluxes for the Atlantic Ocean and Mediterranean Sea Between 1985 and 2018, *Global Biogeochem. Cy.*, 38, e2023GB007862, <https://doi.org/10.1029/2023GB007862>, 2024.
- Planchat, A., Bopp, L., and Kwiatkowski, L.: A fresh look at the pre-industrial air–sea carbon flux using the alkalinity budget, *Biogeosciences*, 22, 6017–6055, <https://doi.org/10.5194/bg-22-6017-2025>, 2025.
- Regnier, P., Resplandy, L., Najjar, R. G., and Ciais, P.: The land-to-ocean loops of the global carbon cycle, *Nature*, 603, 401–410, <https://doi.org/10.1038/s41586-021-04339-9>, 2022.
- Resplandy, L., Hogikyan, A., Müller, J. D., Najjar, R. G., Bange, H. W., Bianchi, D., Weber, T., Cai, W. -J., Doney, S. C., Fennel, K., Gehlen, M., Hauck, J., Lacroix, F., Landschützer, P., Le Quéré, C., Roobaert, A., Schwinger, J., Berthet, S., Bopp, L., Chau, T. T. T., Dai, M., Gruber, N., Ilyina, T., Kock, A., Manizza, M., Lachkar, Z., Laruelle, G. G., Liao, E., Lima, I. D., Nissen, C., Rödenbeck, C., Séférian, R., Toyama, K., Tsujino, H., and Regnier, P.: A Synthesis of Global Coastal Ocean Greenhouse Gas Fluxes, *Global Biogeochem. Cy.*, 38, e2023GB007803, <https://doi.org/10.1029/2023GB007803>, 2024.
- Rödenbeck, C., DeVries, T., Hauck, J., Le Quéré, C., and Keeling, R. F.: Data-based estimates of interannual sea–air CO<sub>2</sub> flux variations 1957–2020 and their relation to environmental drivers, *Biogeosciences*, 19, 2627–2652, <https://doi.org/10.5194/bg-19-2627-2022>, 2022.
- Rustogi, P., Resplandy, L., Liao, E., Reichl, B. G., and Deike, L.: Influence of Wave-Induced Variability on Ocean Carbon Uptake, *Global Biogeochem. Cy.*, 39, e2024GB008382, <https://doi.org/10.1029/2024GB008382>, 2025.
- Sarmiento, J. L., Orr, J. C., and Siegenthaler, U.: A perturbation simulation of CO<sub>2</sub> uptake in an ocean general circulation model, *J. Geophys. Res.-Oceans*, 97, 3621–3645, <https://doi.org/10.1029/91JC02849>, 1992.
- Takahashi, T., Sutherland, S. C., Wanninkhof, R., Sweeney, C., Feely, R. A., Chipman, D. W., Hales, B., Friederich, G., Chavez, F., Sabine, C., Watson, A., Bakker, D. C. E., Schuster, U., Metzl, N., Yoshikawa-Inoue, H., Ishii, M., Midorikawa, T., Nojiri, Y., Körtzinger, A., Steinhoff, T., Hoppema, M., Olafsson, J., Arnarson, T. S., Tilbrook, B., Johannessen, T., Olsen, A., Bellerby, R., Wong, C. S., Delille, B., Bates, N. R., and De Baar, H. J. W.: Climatological mean and decadal change in surface ocean pCO<sub>2</sub>, and net sea–air CO<sub>2</sub> flux over the global oceans, *Deep-Sea Res. Pt. II*, 56, 554–577, <https://doi.org/10.1016/j.dsr2.2008.12.009>, 2009.
- Terhaar, J., Frölicher, T. L., and Joos, F.: Observation-constrained estimates of the global ocean carbon sink from Earth system models, *Biogeosciences*, 19, 4431–4457, <https://doi.org/10.5194/bg-19-4431-2022>, 2022.
- Terhaar, J., Goris, N., Müller, J. D., DeVries, T., Gruber, N., Hauck, J., Perez, F. F., and Séférian, R.: Assessment of Global Ocean Biogeochemistry Models for Ocean Carbon Sink Estimates in RECCAP2 and Recommendations for Future Studies, *J. Adv. Model. Earth Sy.*, 16, e2023MS003840, <https://doi.org/10.1029/2023MS003840>, 2024.
- Wanninkhof, R.: Relationship between wind speed and gas exchange over the ocean, *J. Geophys. Res.*, 97, 7373–7382, <https://doi.org/10.1029/92JC00188>, 1992.
- Wanninkhof, R.: Relationship between wind speed and gas exchange over the ocean revisited, *Limnol. Oceanogr. Meth.*, 12, 351–362, <https://doi.org/10.4319/lom.2014.12.351>, 2014.
- Watson, A. J., Schuster, U., Shutler, J. D., Holding, T., Ashton, I. G. C., Landschützer, P., Woolf, D. K., and Goddijn-Murphy, L.: Revised estimates of ocean-atmosphere CO<sub>2</sub> flux are consistent with ocean carbon inventory, *Nat. Commun.*, 11, 4422, <https://doi.org/10.1038/s41467-020-18203-3>, 2020.
- Weiss, R. F.: Carbon dioxide in water and seawater: the solubility of a non-ideal gas, *Mar. Chem.*, 2, 203–215, [https://doi.org/10.1016/0304-4203\(74\)90015-2](https://doi.org/10.1016/0304-4203(74)90015-2), 1974.
- Weiss, R. F. and Price, B. A.: Nitrous oxide solubility in water and seawater, *Mar. Chem.*, 8, 347–359, [https://doi.org/10.1016/0304-4203\(80\)90024-9](https://doi.org/10.1016/0304-4203(80)90024-9), 1980.
- Zeng, J., Iida, Y., Matsunaga, T., and Shirai, T.: Surface ocean CO<sub>2</sub> concentration and air–sea flux estimate by machine learning with modelled variable trends, *Front. Mar. Sci.*, 9, 989233, <https://doi.org/10.3389/fmars.2022.989233>, 2022.